CrystEngComm

Accepted Manuscript

ROYAL SOCIETY OF CHEMISTRY

www.rsc.org/crystengcomm

Journal Name

COMMUNICATION

Facile template-free approach for fabrication of flower-like CdS: the evolutionary process of the structure and the performance of photocatalytic activity†

Received 00th January 20xx,
Accepted 00th January 20xx

DOI: 10.1039/x0xx00000x

www.rsc.org/

Weizhi Wang,*[a] Yajing Lu,[a] Yafei Xu,[a] Konglin Wu,[a] Jiarui Huang,[a] Changchun Ji [a] and Si Ok Ryu*[b]

Uniform flower-like CdS was fabricated successfully using a facile hydrothermal approach without templates or additives. The formation process of the flower-like structures was investigated in detail. The as-prepared flower-like CdS exhibited good photocatalytic activity for the photodegradation of various organic dyes.

Semiconductor photocatalysts technology has been considered a promising strategy to solve environmental issues through the photodegradation of organic pollutants because it is an eco-friendly, low-cost and sustainable treatment.[1] For example, anatase TiO_2 is the most studied semiconductor as an environmental cleanup photocatalyst owing to its photoactivity, stability, biocompatibility, and low cost.[2-4] On the other hand, TiO_2 has a high band gap and responds to UV light only.[1] Therefore, TiO_2 can only utilize a small part (< 5%) of the solar spectrum, which limits its practical application as photocatalyst. Therefore, considerable efforts have been made to find efficient photocatalysts that can effectively degrade organic pollutants under visible light irradiation. As an important II-VI semiconductor, cadmium sulfide (CdS) is an ideal visible light driven photocatalyst because of its narrow and direct band gap (at room temperature is approximately 2.42 eV), which corresponds well to the solar spectrum. Therefore, CdS has been extensively studied in diverse photocatalytic fields such as reduction of nitro organics, water splitting and dye degradation.[5-8]

The morphology and size of the semiconductor catalyst has a great effect on the photocatalytic activity because the reactants are in contact with the photocatalyst surface, where the catalytic reaction takes place. For CdS nanostructures, the morphology and size play important roles in the optical and physical properties.[9] Therefore, chemists and material scientists have made considerable efforts to control the morphology and size of CdS nanomaterials, and a range of CdS nanostructures have been obtained, such as quantum dots,[10, 11] nanospheres,[12, 13] nanorods,[13, 14] nanowires,[15, 16] nanobelts,[17, 18] nanosheets,[19] nanotubes,[20] nanoboxes,[21] hierarchical nanostructures,[22-26] hollow nanostructures,[27, 28] and flower-like nanostructure.[8, 29] To fabricate CdS nanostructures with the desired morphology and different size, various synthetic approaches have been developed, such as chemical vapor deposition,[30] thermal evaporation,[31] thermal decomposition,[32, 33] vapor–liquid–solid process,[18, 34] electrodeposition,[16] template method,[21, 35] microwave-assisted aqueous synthesis,[36] solvothermal synthesis,[37-39] and hydrothermal method.[29, 40-42] In these, the hydrothermal method has been demonstrated to be an effective approach for fabricating CdS nanomaterials. For example, Masoud et al. have reported the size-controlled synthesis of CdS nanostructure by a mild and simple hydrothermal method.[29]

Herein, we show a facile hydrothermal approach to synthesize flower-like CdS nanomaterials with uniform size and good dispersibility. The as-prepared flower-like CdS is composed of small CdS nanocrystals with high crystalline quality. The formation of the flower-like structure does not require a surfactant, assistant reagent or a template. Moreover, there are gaps between the small CdS nanocrystals, resulting in the presence of interstices inside the products. This is different from common flower-like or spherical CdS nanomaterials with close and solid structures.[8, 36, 38, 43-45] This study examined the structural evolution of the product in detail and proposed the formation process of the flower-like CdS. The photocatalytic performance of the products was also evaluated by the degradation of several organic dyes under visible light irradiation. The results show that the as-prepared flower-like CdS is an efficient photocatalyst and is potentially useful for applications in waste water treatment.

The panoramic morphology and size of the as-prepared products were examined by field emission scanning electron microscopy (FESEM). A general overview FESEM image (Fig. 1a)

[a] The Key Laboratory of Functional Molecular Solids, Ministry of Education, Anhui Laboratory of Molecular-Based Materials, College of Chemistry and Materials Science, Anhui Normal University, Wuhu 241000, P.R. China. E-mail: wangwz@mail.ahnu.edu.cn
[b] School of Chemical Engineering, Yeungnam University, Gyeongsan, Gyeoungbuk 712749, R. Korea. E-mail: soryu@ynu.ac.kr

† Electronic supplementary information (ESI) available: Experimental procedures, Fig. S1 , S2 and S3. See DOI: 10.1039/x0xx00000x

shows that the products are particles with a rough surface. These particles are almost uniform size with a diameter of approximately 110 nm. The high magnification FESEM image (Fig. 1b) shows that the products are formed from aggregated smaller particles with a flower-like structure, which is consistent with the rough surface observed in Fig 1a. The phase of the products was examined by powder X-ray diffraction (XRD). The diffraction peaks of the XRD pattern could be indexed to hexagonal CdS (see Fig. 1c) with calculated lattice constants of a = b = 4.148 Å and c = 6.712 Å; these values are in agreement with the literature values of 4.140 and 6.719 Å, respectively (JCPDS Card File No. 41-1049). In addition, the peaks at 26.6°, 43.8°, 52.1°, and 54.6°, correspond to the (111), (220), (311), and (222) planes of the cubic CdS (JCPDS Card File No. 10-0454) with calculated lattice constant of a = 5.822 Å. It indicates that the wurtzite (WZ) and zinc blende (ZB) phases coexist in the products. Existence of two phases of crystal structure is common in binary semiconductors such as CdS, CdSe and ZnS, etc.[8, 46] Fig 1d shows the energy dispersive X-ray (EDX) spectrum of the products, which indicates that Cd and S atomic ratio are close to stoichiometric CdS (the Cu peaks came from the copper film substrate). These results reveal that uniform flower-like CdS had been fabricated using a facile hydrothermal approach.

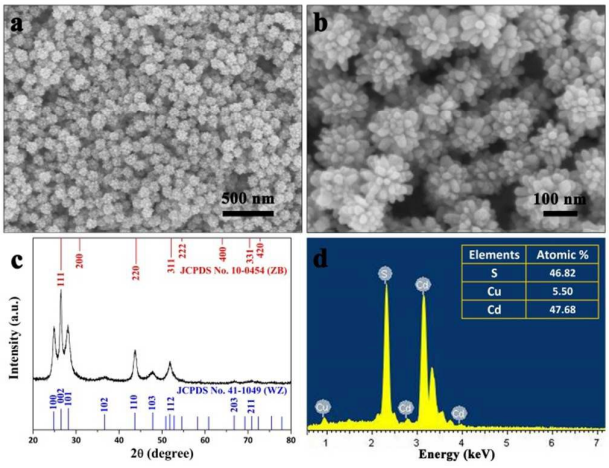

Fig. 1 Morphology and phase of the as-prepared products: (a) general view and (b) magnified FESEM image of the products. (c) XRD pattern and (d) EDX spectrum of the as-prepared products.

The structure of the products was examined by transmission electron microscopy (TEM) and high resolution transmission electron microscopy (HRTEM) in more detail. Fig. 2a and b show that the products have a flower-like structure with good dispersibility and an almost uniform size. The high magnification TEM images show that the flower-like products are composed of some smaller particles (Fig. 2c and d). The diameter of the smaller particles is approximately 15 nm. The microstructural features of the smaller particles were demonstrated more clearly by HRTEM (Fig. 2e and f). The two sets of fringe spacing of the lattice planes observed in the middle right of the Fig. 2e are 3.37 and 3.12 Å, which correspond to the (002) and (101) lattice planes of the hexagonal CdS, respectively. At the top left of the Fig. 2e, the lattice spacing of 3.37 Å could be ascribed to the (111) plane of the cubic CdS. Existence of WZ phase and ZB phase is consistent with the result obtained from XRD. The ring-like selected area electron diffraction (SAED) pattern (inset of Fig. 2f) taken from an entire flower-like CdS indicates the polycrystalline nature of the products. The HRTEM images and the SAED pattern further demonstrate that the as-prepared flower-like CdS were formed from the aggregation of high crystalline CdS nanocrystals. Interestingly, the as-prepared flower-like CdS are not a solid structure. A dark/light contrast can be observed clearly inside the products from the TEM images, which reveals that the smaller CdS nanocrystals are not densely aggregated to form a flower-like structure, resulting in the presence of inner interstices.

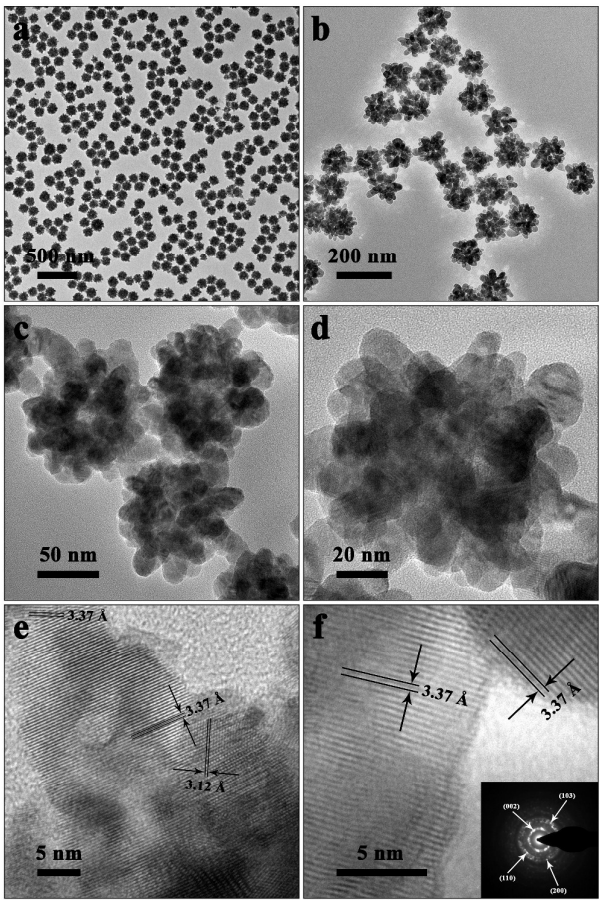

Fig. 2 (a, b) Typical and (c, d) magnified TEM image of the flower-like CdS. (e, f) HRTEM images of the CdS nanocrystals that compose the flower-like products. Inset of (f): SAED pattern of the products.

Nitrogen adsorption and desorption measurements were further performed to examine the inner architectures and the specific surface area of the as-prepared flower-like CdS. As shown in Fig. 3, the adsorption-desorption isotherm of the products exhibits a hysteresis loop at p/p_0 ranges of 0.7 to 0.98.

According to IUPAC classification such isotherm shape can be categorized as type IV, which is characteristic of mesoporous materials. The Brunauer-Emmett-Teller (BET) surface area of the flower-like CdS was calculated as 47.2 m^2g^{-1}. Furthermore, the inset of Fig. 3 shows the pore size distribution of the products. Using the desorption branch of the nitrogen isotherm and the Barett-Joyner-Halenda (BJH) method, the pore size distribution indicates that the as-prepared flower-like CdS has an average pore diameter of 11.3 nm.

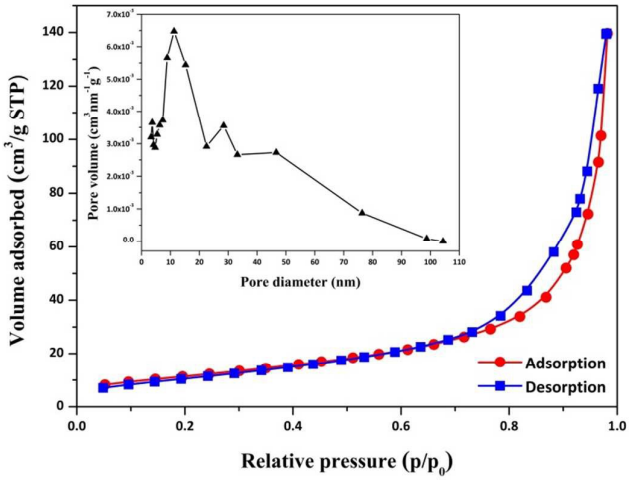

Fig. 3 Nitrogen adsorption-desorption isotherm of the flower-like CdS. The inset is the corresponding pore size distribution.

The above analyses reveal that the uniform flower-like CdS nanomaterials with inner interstices can be fabricated by a facile hydrothermal approach. Since no any toxic additives or templates are added, this approach is more eco-friendly in comparison with other methods.[36]

To investigate the formation process of the as-prepared flower-like CdS, we examined the products obtained at different reaction stages. Fig. 4a-h shows a set of TEM images corresponding to the products obtained at different reaction times. After a short reaction time for 0.5 h, a large number of dispersive spherical products were obtained (Fig. 4a). The high magnification TEM image (Fig. 4b) shows that the surface of the spherical products was not smooth, and there were no obvious interstices inside the products. When the reaction time was 1 h, the structure of the products was still spherical (Fig. 4c), but the dark/light contrast of the inner section of the spherical products indicated that interior interstices had begun to appear. Moreover, the surface of the products became rougher than the products obtained at 0.5 h (Fig. 4d). The distinction of the surface between these two products can be observed clearly in the SEM images of the products (Fig. S1a and b). Sharp, strong and readily identifiable diffraction peaks cannot be observed in the XRD patterns of the two products (Fig. S1g), suggest that crystalline CdS was not formed in a short reaction time. As the reaction time was extended to 2 h, the morphology of the products transformed from a spherical to a flower-like structure consisting of aggregative particles, and the interstices between the particles could be observed clearly (Fig. 4e and f). The XRD pattern shows that the products are crystalline CdS nanomaterials (Fig. S1g). When the reaction time was 3 h, the interior interstices of the flower-like products became more distinct (Fig. 4g and h). The morphology and crystallinity of the products (Fig. S1d and g) were close to the products of the typical experiment obtained at 4 h. During longer reaction time up to 12 h, the morphology, size and crystallinity of the products did not change noticeably but appeared similar to the typical products, as indicated by SEM, TEM and XRD (Fig. S1e-g). Therefore, 4 h was chosen as the optimal reaction time for the fabrication of the flower-like CdS.

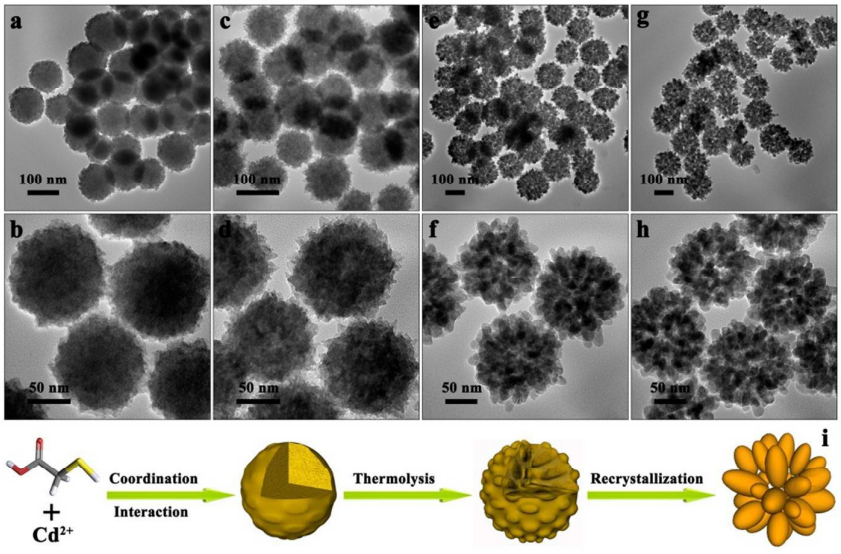

Fig. 4 Images of the products, showing the formation process of the flower-like CdS. TEM images of the products obtained after reaction times of (a-b) 0.5, (c-d) 1, (e-f) 2, and (g-h) 3 h. (i) Schematic illustration of the formation process of the flower-like CdS.

Journal Name

COMMUNICATION

Based on the above experimental results, the formation process of the flower-like CdS is proposed. In our reaction system, thioglycollic acid (TGA) was chosen to react with Cd^{2+} ions. Previous studies have demonstrated that the thiol groups and the carboxylic groups in mercaptocarboxylic acid have a strong tendency to coordinate with Cd^{2+} ions.[47, 48] Therefore, Cd-TGA complexes were formed first through the coordination interaction between Cd^{2+} and TGA.[49] In a short time, the Cd-TGA complexes aggregated into dispersive spherical structures driven by the minimization of the interfacial energy and the surface to volume ratio.[50] Subsequently, at high pH and hydrothermal conditions, the coordination interaction between Cd^{2+} and TGA broke down with the release of sulfur,[29, 51] resulting in the formation of amorphous CdS. Owing to the decomposition of the Cd-TGA complexes, the surface of the products became rougher and the internal structure began to loosen, as shown in Fig. 4c and d. Because larger crystallites are thermodynamically favored,[52] highly crystalline CdS nanocrystals were formed through a recrystallization process (i.e., Ostwald ripening) with increasing hydrothermal time, resulting in the appearance of interstices inside the products. Finally, the flower-like products consisting of high crystalline CdS nanocrystals could be obtained. Fig. 4i shows a schematic illustration of the above formation processes.

In view of most catalytic reactions occur on the catalyst surface,[53, 54] the presence of inner interstices is conducive to improving the photocatalytic activity of the products due to the increase in surface area. We investigated the optical properties of the flower-like CdS by UV-vis absorption at room temperature to evaluate the quality of the products as a photocatalyst. The UV-vis spectrum (Fig. 5a) shows that the flower-like CdS have an absorption in the visible region between 450 nm to 520 nm with a maximum absorption at ~490 nm. Based on the UV-vis spectrum, the band gap of the products can be obtained using Tauc's equation: $(\alpha h\nu)^{1/n} = A(h\nu - Eg)$,[55] where α, $h\nu$, A, and Eg are the absorption coefficient, photon energy, constant, and band gap, respectively. The value of the exponent n is 1/2 because CdS is a direct transition semiconductor. The Eg of the flower-like CdS is approximately 2.29 eV according to the $(\alpha h\nu)^2$ vs $h\nu$ curve of the products (inset of Fig. 5a). The transient photocurrent response of the products was measured in a standard three-electrode system under visible light irradiation. The as-prepared flower-like CdS was spread onto indium-tin oxide (ITO) conductor glass as working electrode. In the dark, no photocurrent was observed for both the flower-like CdS and blank ITO. In contrast, the flower-like CdS showed appreciable photocurrents under visible light irradiation. As shown in Fig. 5b, the spikes of transient photocurrent responses of the products over on-off cycles of intermittent light irradiation are observed with good reproducibility. It is generally believed that the photocurrent mainly originates form the diffusion of the photogenerated electrons to the back contact and meanwhile the photoinduced holes are taken by the hole acceptor in the electrolyte. Therefore, the fast and uniform transient photocurrent response of the products indicates efficient separation of photoexcited electron-hole pairs from the as-prepared flower-like CdS under visible light irradiation.[56]

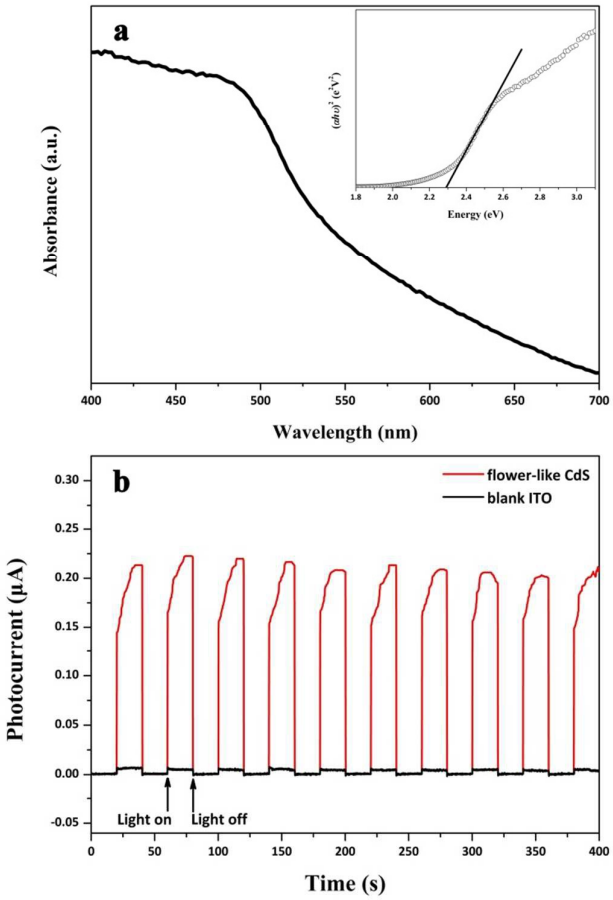

Fig. 5 (a) UV-vis spectrum and $(\alpha h\nu)^2$ vs. $h\nu$ curve (inset) of the flower-like CdS. (b) Transient photocurrent response of the flower-like CdS and blank ITO.

The above characterization and analyses demonstrate that the as-prepared flower-like CdS is suitable to act as a visible light responsive photocatalyst. To evaluate the photocatalytic activity of the products, the photodegradation of methylene blue (MB) was examined under visible light irradiation. In the

presence of the flower-like CdS, the color of the aqueous MB solution changed gradually from blue to colorless during the irradiation process. Fig. 6a shows the temporal evolution of the absorption spectra of the MB solution at various irradiation times in the presence of the products. Along with the extension of irradiation time, the intensity of the characteristic absorption peak of MB at 660 nm decreased continually to nearly disappeared, moreover, there's no new absorption bands appeared. This indicates the MB was photodegraded.[57] Fig. 6b presents a plot of the concentration changes in MB (C_t/C_0) as a function of the irradiation time. Here, C_t and C_0 are the initial concentration and the degradation process concentration of MB, respectively, which was determined by the absorption value at 660 nm. Negligible degradation of MB was detected in light irradiation without a photocatalyst or in the dark with the flower-like CdS. In contrast, obvious degradation of MB was observed under light irradiation in the presence of flower-like CdS. Approximately 82% of MB was photodegraded within 90 min of irradiation and was almost degraded completely after 150 min.

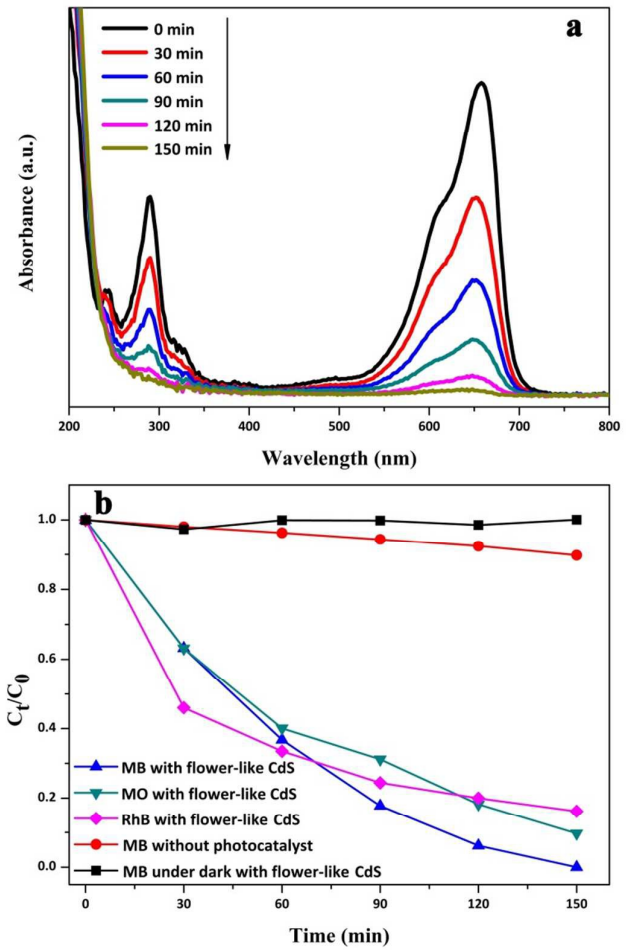

Fig. 6 (a) Temporal UV-vis absorption spectra of MB in the presence of flower-like CdS under visible light irradiation. (b) Degradation efficiency of MB under different conditions, and photodegradation efficiency of MO and RhB.

To further demonstrate the photodegradation performance of the flower-like CdS, the photocatalytic degradation of methyl orange (MO) and rhodamine B (RhB) were also conducted. The adsorption spectra show that the characteristic absorption peaks corresponding to MO and RhB, at 462 and 550 nm, decreased gradually with the extension of the irradiation time in the presence of the flower-like CdS (Fig. S2). Fig. 6b also presents the concentration changes of MO and RhB (C_t/C_0) as a function of the irradiation time. After 150 min irradiation, 91% of MO was degraded. For RhB, about 85% could be reached in the same period. The different degradation results can be attributed to the dissimilar adsorption characteristic of the different organic dyes on the flower-like CdS.[58] Overall, the above results demonstrate that the as-prepared flower-like CdS has good photocatalytic activity for various organic dyes, which could be attributed to the large surface area and good crystallinity.[45]

To evaluate the stability of the as-prepared flower-like CdS, the photodegradation of MB was repeated for several cycles. In the recycled procedure, all processes and conditions remain the same. As shown in Fig. 7, although the photocatalytic activity of the products decreased after 10 h of visible light irradiation, 80 % of photocatalytic activity still remained. In addition, the XRD patterns of the recycled flower-like CdS are shown in Fig. S3a, which indicates that the phase and the crystallinity of the products remain intact. The FESEM and TEM images of the recycled products (Fig. S3b-i) reveal that small CdS nanocrystals that compose the flower-like structure were gradually separated from each other during recycled photocatalytic process. The change of morphology and the photocorrosion of CdS during the photocatalytic process were supposed to the reasons for the decreased photocatalytic activity of the products.[59]

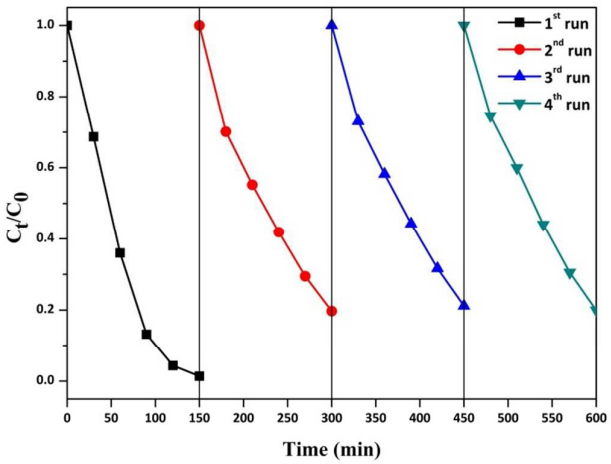

Fig. 7 Cyclic test of photocatalytic degradation of MB for the flower-like CdS under visible light irradiation.

Conclusions

In summary, we demonstrated a facile hydrothermal approach for the fabrication of uniform flower-like CdS without any

templates or additives. The as-prepared flower-like CdS consisted of high crystalline CdS nanocrystals, and there were interstices inside the products. A series of intermediate morphologies were observed during the formation of the flower-like products. Based on the experimental results, a process of structural evolution, from the spherical Cd-TGA complexes to the flower-like CdS, was proposed to explain the formation of the products. Furthermore, the investigation of the photocatalytic properties showed that the flower-like CdS possess good photocatalytic activity for the degradation of various organic dyes under visible light irradiation. This study presents a new paradigm for the fabrication of metal sulfide nanostructure and the as-prepared flower-like CdS has potential applications to the treatment of organic pollutants in waste water.

Acknowledgements

This research was supported by the National Natural Science Foundation of China (No. 21201008, 21501004, 21471005), Anhui Provincial Natural Science Foundation (No. 1208085QB31, 1408085MB32) and Science Foundation for The University Outstanding Young Talent of Anhui Province (No. 2013SQRL012ZD). Moreover, we appreciate Xiaoyao Xi from School of Journalism and Communication, Anhui Normal University, for drawing the illustration.

Notes and references

1 R. Asahi, T. Morikawa, T. Ohwaki, K. Aoki and Y. Taga, *Science*, 2001, **293**, 269-271.
2 T. Y. Ke, C. W. Peng, C. Y. Lee, H. T. Chiu and H. S. Sheu, *CrystEngComm*, 2009, **11**, 1691-1695.
3 Y. Aoyama, Y. Oaki, R. Ise and H. Imai, *CrystEngComm*, 2012, **14**, 1405-1411.
4 X. X. Yao, X. H. Liu, T. Y. Liu, K. Wang and L. D. Lu, *CrystEngComm*, 2013, **15**, 10246-10254.
5 Q. Li, X. Li, S. Wageh, A. A. Al-Ghamdi and J. G. Yu, *Adv. Energy Mater.*, 2015, **5**, 1500010.
6 F. K. Ma, G. Zhao, C. Li, T. L. Wang, Y. Z. Wu, J. X. Lv, Y. Y. Zhong and X. P. Hao, *CrystEngComm*, 2016, **18**, 631-637.
7 S. S. Warule, N. S. Chaudhari, R. T. Shisode, K. V. Desa, B. B. Kale and M. A. More, *CrystEngComm*, 2015, **17**, 140-148.
8 Q. Z. Wang, J. H. Lian, J. J. Li, R. F. Wang, H. H. Huang, B. T. Su and Z. Q. Lei, *Sci. Rep.*, 2015, **5**, 13593.
9 A. B. Panda, G. Glaspell and M. S. El-Shall, *J. Am. Chem. Soc.*, 2006, **128**, 2790-2791.
10 M. Naito, K. Iwahori, A. Miura, M. Yamane and I. Yamashita, *Angew. Chem., Int. Ed.*, 2010, **49**, 7006-7009.
11 J. S. Zheng, F. Huang, S. G. Yin, Y. J. Wang, Z. Lin, X. L. Wu and Y. B. Zhao, *J. Am. Chem. Soc.*, 2010, **132**, 9528-9530.
12 Y. M. Guo, J. F. Wang, Z. K. Tao, F. F. Dong, K. Wang, X. M. Ma, P. H. Yang, P. P. Hu, Y. T. Xu and L. Yang, *CrystEngComm*, 2012, **14**, 1185-1188.
13 T. Shanmugapriya, R. Vinayakan, K. G. Thomas and P. Ramamurthy, *CrystEngComm*, 2011, **13**, 2340-2345.
14 C. C. Kang, C. W. Lai, H. C. Peng, J. J. Shyue and P. T. Chou, *ACS Nano*, 2008, **2**, 750-756.
15 S. L. Xiong, B. J. Xi, C. M. Wang, G. F. Zou, L. F. Fei, W. Z. Wang and Y. T. Qian, *Chem. -Eur. J.*, 2007, **13**, 3076-3081.
16 D. S. Xu, Y. J. Xu, D. P. Chen, G. L. Guo, L. L. Gui and Y. Q. Tang, *Adv. Mater.*, 2000, **12**, 520-522.
17 L. F. Dong, J. Jiao, M. Coulter and L. Love, *Chem. Phys. Lett.*, 2003, **376**, 653-658.
18 L. Li, P. C. Wu, X. S. Fang, T. Y. Zhai, L. Dai, M. Y. Liao, Y. Koide, H. Q. Wang, Y. Bando and D. Golberg, *Adv. Mater.*, 2010, **22**, 3161-3165.
19 Y. Xu, W. W. Zhao, R. Xu, Y. M. Shi and B. Zhang, *Chem. Commun.*, 2013, **49**, 9803-9805.
20 X. Kuang, Y. Ma, C. Y. Zhang, H. Su, J. Zhang and B. Tang, *Chem. Commun.*, 2015, **51**, 5955-5958.
21 M. R. Kim and D. J. Jang, *Chem. Commun.*, 2008, 5218-5220.
22 S. L. Xiong, X. G. Zhang and Y. T. Qian, *Cryst. Growth Des.*, 2009, **9**, 5259-5265.
23 C. Z. Wang, E. F. Yifeng, L. Z. Fan, Z. H. Wang, H. B. Liu, Y. L. Li, S. H. Yang and Y. L. Li, *Adv. Mater.*, 2007, **19**, 3677-3681.
24 Z. Yu, X. Wu, J. Wang, W. N. Jia, G. S. Zhu and F. Y. Qu, *Dalton Trans.*, 2013, **42**, 4633-4638.
25 H. X. Niu, Q. Yang, K. B. Tang, Y. Xie and Y. C. Zhu, *J. Nanosci. Nanotechnol.*, 2006, **6**, 162-167.
26 F. Y. Sun, Q. Yang, D. L. Zhao and Y. Wu, *J. Electron. Mater.*, 2007, **36**, 1567-1573.
27 J. X. Huang, Y. Xie, B. Li, Y. Liu, Y. T. Qian and S. Y. Zhang, *Adv. Mater.*, 2000, **12**, 808-811.
28 X. Y. Ma, X. L. Zhang, J. Gong, N. Wang, B. Fan and L. Y. Qu, *CrystEngComm*, 2012, **14**, 246-250.
29 M. Salavati-Niasari, F. Davar and M. R. Loghman-Estarki, *J. Alloys Compd.*, 2009, **481**, 776-780.
30 R. B. Liu, Z. A. Li, C. H. Zhang, X. X. Wang, M. A. Kamran, M. Farle and B. S. Zou, *Nano Lett.*, 2013, **13**, 2997-3001.
31 T. Y. Zhai, X. S. Fang, Y. Bando, B. Dierre, B. D. Liu, H. B. Zeng, X. J. Xu, Y. Huang, X. L. Yuan, T. Sekiguchi and D. Golberg, *Adv. Funct. Mater.*, 2009, **19**, 2423-2430.
32 G. Z. Shen and C. J. Lee, *Cryst. Growth Des.*, 2005, **5**, 1085-1089.
33 T. Trindade and P. OBrien, *J. Mater. Chem.*, 1996, **6**, 343-347.
34 Z. X. Yang, W. Zhong, P. Zhang, M. H. Xu, C. T. Au and Y. W. Du, *CrystEngComm*, 2012, **14**, 585-589.
35 Y. J. Xiong, Y. Xie, J. Yang, R. Zhang, C. Z. Wu and G. Du, *J. Mater. Chem.*, 2002, **12**, 3712-3716.
36 C. H. Deng and X. B. Tian, *Mater. Res. Bull.*, 2013, **48**, 4344-4350.
37 K. B. Tang, Y. T. Qian, J. H. Zeng and X. G. Yang, *Adv. Mater.*, 2003, **15**, 448-450.
38 Y. M. Guo, J. F. Wang, L. Yang, J. Zhang, K. Jiang, W. J. Li, L. L. Wang and L. L. Jiang, *CrystEngComm*, 2011, **13**, 5045-5048.
39 F. Gao, Q. Y. Lu, S. H. Xie and D. Y. Zhao, *Adv. Mater.*, 2002, **14**, 1537-1540.
40 P. W. Dunne, C. L. Starkey, M. Gimeno-Fabra and E. H. Lester, *Nanoscale*, 2014, **6**, 2406-2418.
41 Y. X. Li, L. F. Tang, S. Q. Peng, Z. C. Li and G. X. Lu, *CrystEngComm*, 2012, **14**, 6974-6982.
42 H. Q. Cao, G. Z. Wang, S. C. Zhang, X. R. Zhang and D. Rabinovich, *Inorg. Chem.*, 2006, **45**, 5103-5108.
43 A. Phuruangrat, N. Ekthammathat, T. Thongtem and S. Thongtem, *J. Alloys Compd.*, 2011, **509**, 10150-10154.
44 Z. F. Zhu, Y. F. Wu, H. Liu, G. H. Chen and C. K. Zhu, *Mater. Lett.*, 2013, **107**, 90-92.
45 Z. Yu, B. S. Yin, F. Y. Qu and X. Wu, *Chem. Eng. J.*, 2014, **258**, 203-209.
46 C. C. Chen, A. B. Herhold, C. S. Johnson and A. P. Alivisatos, *Science*, 1997, **276**, 398-401.
47 J. C. Bayon, M. C. Brianso, J. L. Brianso and P. G. Duarte, *Inorg. Chem.*, 1979, **18**, 3478-3482.
48 I. G. Dance, M. L. Scudder and R. Secomb, *Inorg. Chem.*, 1983, **22**, 1794-1797.
49 H. J. Niu and M. Y. Gao, *Angew. Chem., Int. Ed.*, 2006, **45**, 6462-6466.
50 Y. W. Wang, J. T. He, C. C. Liu, W. H. Chong and H. Y. Chen, *Angew. Chem., Int. Ed.*, 2015, **54**, 2022-2051.

51 N. Mahapatra, S. Panja, A. Mandal and M. Haider, *J. Mater. Chem. C*, 2014, **2**, 7373-7384.
52 W. L. Noorduin, E. Vlieg, R. M. Kellogg and B. Kaptein, *Angew. Chem., Int. Ed.*, 2009, **48**, 9600-9606.
53 J. Wintterlin, S. Volkening, T. V. W. Janssens, T. Zambelli and G. Ertl, *Science*, 1997, **278**, 1931-1934.
54 X. L. Zhou, J. Jiang, T. Ding, J. J. Zhang, B. C. Pan, J. Zuo and Q. Yang, *Nanoscale*, 2014, **6**, 11046-11051.
55 J. Tauc, in *Optical properties of solids*, ed. F. Abelès, North-Holland Pub. Co., Amsterdam, 1972, p. 372.
56 S. Q. Liu, Z. Chen, N. Zhang, Z. R. Tang and Y. J. Xu, *J. Phys. Chem. C*, 2013, **117**, 8251-8261.
57 J. S. Hu, L. L. Ren, Y. G. Guo, H. P. Liang, A. M. Cao, L. J. Wan and C. L. Bai, *Angew. Chem., Int. Ed.*, 2005, **44**, 1269-1273.
58 S. B. Khan, M. Faisal, M. M. Rahman and A. Jamal, *Sci. Total Environ.*, 2011, **409**, 2987-2992.
59 J. Z. Chen, X. J. Wu, L. S. Yin, B. Li, X. Hong, Z. X. Fan, B. Chen, C. Xue and H. Zhang, *Angew. Chem., Int. Ed.*, 2015, **54**, 1210-1214.

Table of Contents

Uniform flower-like CdS with inner interstices can be fabricated by a facile hydrothermal approach, which has good photocatalytic activity.